

A98-37361

AIAA-98-4284

TRAJECTORIES TO JUPITER VIA GRAVITY ASSISTS FROM VENUS, EARTH, AND MARS

Anastassios E. Petropoulos*, James M. Longuski† and Eugene P. Bonfiglio‡
*School of Aeronautics and Astronautics, Purdue University,
West Lafayette, Indiana 47907-1282*

Abstract

Gravity-assist trajectories to Jupiter, launching between 1999 and 2031, are identified using patched-conic techniques. The classical trajectories, such as the Venus-Earth-Earth gravity assist (VEEGA), and many less conventional paths, such as Venus-Mars-Venus-Earth, are examined. Flight times of up to about seven years are considered. The ΔV -optimized results confirm that VEEGAs are the most effective gravity-assist trajectory type. If the Earth is excluded as a flyby body, Venus-Venus-Venus gravity assists are typically the best option, although at times non-conventional paths are better. These non-conventional paths can occasionally decrease the time of flight significantly, at very minor ΔV cost, when compared to the classical types.

Introduction

Since Galileo Galilei pointed his tiny telescope at Jupiter and discovered its four moons in 1610, our largest planet has fascinated astronomers and laymen alike. Four flyby spacecraft (Pioneers 10 and 11, and Voyagers 1 and 2) have reconnoitered this miniature solar system; and now, at the time of this writing, the Galileo spacecraft is orbiting the planet and performing detailed surveys of its atmosphere, satellites and magnetosphere. There have been many wonderful discoveries, and as the Galileo project completes its extended mission, the Jovian system beckons for further exploration. The mounting evidence of liquid water below the icy surface of Europa offers the tantalizing possibility of life — spurring NASA to plan a Europa orbital mission to examine this satellite more closely in the next decade.

With these plans for a sixth mission on the drawing board, it seems highly likely that scientific interest in Jupiter will continue to increase. At the same time, budget constraints and the NASA mandate of “better, cheaper, faster” demand that creative solutions be found, if we are to maintain a vigorous program of exploration of Jupiter.

The most potent way of reducing launch costs (which are among the most expensive) is to use the

proven technique of gravity assist. Voyager 2 used gravity assists from Jupiter, Saturn, and Uranus, to eventually reach Neptune in 12 years; Galileo used a VEEGA (Venus Earth Earth Gravity Assist) to reach Jupiter in just over 6 years. Unfortunately, gravity-assist trajectories usually require long flight times, which can drive up mission operations costs. However, with the development of more autonomous spacecraft and more efficient operations procedures, these costs are expected to decrease steadily. Until other means of space transportation become readily available (electric propulsion, solar sails, aerogravity assist, or warp drive!), the gravity assist option will, in spite of the flight time issue, remain the most attractive alternative. (And even as other propulsive technologies emerge, they will gain considerable augmentation when coupled with gravity assist.)

The principle of gravity assist has been understood since the 19th century when Leverrier (see Broucke¹) and Tisserand (see Battin²) explained large perturbations of the orbits of comets by the planet Jupiter. In the late 1950s, Battin³ considered the use of the gravitational attraction of a planet to place a spacecraft on the return leg of its round-trip interplanetary journey. The former Soviet Union used lunar gravitational attraction to obtain desirable return trajectories.⁴ Many investigators in the early 1960s explored the enormous potential of the gravitational swingby maneuver, including Deewester,⁵ Flandro,⁶ Gillespie *et al.*,⁷ Hollister,⁸ Minovitch,⁹ Niehoff,¹⁰ Ross,¹¹ Sohn,¹² and Sturms and Cutting.¹³

Stancati *et al.*¹⁴ demonstrate that VEGA (Venus Earth Gravity Assist) and ΔV -EGA (Delta-V Earth

*Doctoral Candidate, Member AIAA.

†Professor, Associate Fellow AIAA, Member AAS.

‡Graduate Student.

Copyright © 1998 by Anastassios E. Petropoulos, James M. Longuski and Eugene P. Bonfiglio. Published by the American Institute of Aeronautics and Astronautics, Inc. with permission.

Gravity Assist) trajectories to the outer planets (including Jupiter) provide two to three times the net payload capability of direct transfers. A definitive study of VEGA and VEEGA trajectories to Jupiter, Saturn, and selected comets for launches in the last decade of the twentieth century is presented by Diehl and Myers.¹⁵ Ten mission designers spent several months in the effort.

In order to speed up the search for gravity-assist trajectories, Williams¹⁶ developed automated design software based on the JPL (Jet Propulsion Laboratory) interactive program STOUR¹⁷ (Satellite Tour Design Program). The new version is capable of finding all patched-conic, gravity-assist trajectories for a given set of launch dates and launch V_∞ s under a given maximum TOF (time of flight). Patel added¹⁸ the capability of including ΔV s between gravity assists, and (with Longuski) demonstrated¹⁹ the program's ability to automatically find all of the VEGA and VEEGA trajectories discovered by Diehl and Myers, plus a few more. Later, Staugler²⁰ incorporated an algorithm to automatically design V_∞ -leveraging trajectories (including ΔV -EGAs).

In this paper we use STOUR to identify gravity-assist trajectories via Venus, Earth, and Mars to Jupiter during a three decade launch period from 1999 to 2031. We are interested in low launch energy trajectories with low total ΔV and with reasonable TOFs (less than about 7 years). For selected cases we find the ΔV -optimal solutions using the JPL software MIDAS²¹ (Mission Analysis and Design Software). Since we are considering up to four gravity assists with three of the inner planets, there are 120 possible paths (or combinations). Although STOUR

is a very powerful tool, it takes several days (on a Sun UltraSPARC 1 workstation) to assess one path (*e.g.* VEEGA) for a three decade launch period. Thus it is impractical to merely grind through all possible combinations, and so — as is often the case — engineering judgement and analysis are required. We find the simple analytic techniques developed by Hollenbeck²² very helpful in predicting the potential performance of combinations of Venus and Earth gravity assists. Further refinements of these techniques are given by Sims,²³ a detailed analysis of ΔV -EGA trajectories is presented by Sims *et al.*²⁴ We show that extending this concept to include up to four gravity assists gives deep insight into which paths are likely to be effective and which ineffective. We call the problem of selection, pathfinding, and it is the central issue of multiple gravity-assist mission design.

Classical Trajectories

Certain highly effective trajectory types have been well known and commonly used in mission planning, thus meriting the name "classical." Specifically, in this paper the classical trajectories will be taken as ΔV -EGA, VEGA, VEEGA, V^2 , and V^3 , where V^n denotes n Venus gravity assists after Earth launch.

The ΔV -EGA is a V_∞ -leveraging trajectory in which a maneuver (ΔV) is performed near apoapsis after Earth launch, such that the spacecraft re-encounters Earth with a higher V_∞ for the final gravity assist. (This describes the exterior ΔV -EGA for heliocentrically outbound spacecraft. The symmetric case, where the spacecraft is inbound, is termed interior.)

In the case of VEGA, VEEGA, and V^n trajectories to Jupiter, the disadvantage of launching into a lower energy orbit in order to reach the first Venus is more than offset by the benefit of a high V_∞ at a body that is almost as massive as the Earth. In fact, for typical launch V_∞ s, the V_∞ at Venus is so high that a single flyby of the planet cannot turn the V_∞ enough to reach Jupiter. A second flyby of Venus is also insufficient, but can be adequately augmented with a maneuver during or after the flyby. A third Venus flyby can alleviate the need for the maneuver. The VEGAs and VEEGAs are more effective from an energy standpoint not only because the Earth can provide slightly more V_∞ turning, but also because after the Venus flyby we no longer need to maintain a perihelion distance as low as Venus's orbit. V_∞ -leveraging can often be effectively incorporated into paths with repeated flybys of the same body.

A salient feature of the classical trajectories, which accounts for their common use, is the fact that

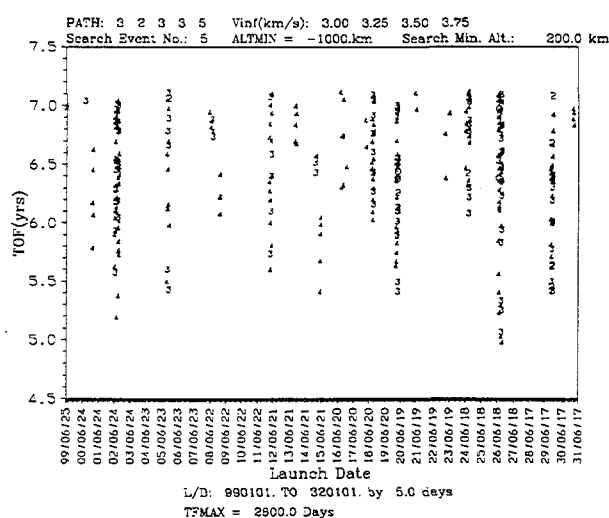


Fig. 1 Resonant and non-resonant, low launch energy VEEGAs with arrival $V_\infty < 8$ km/s.

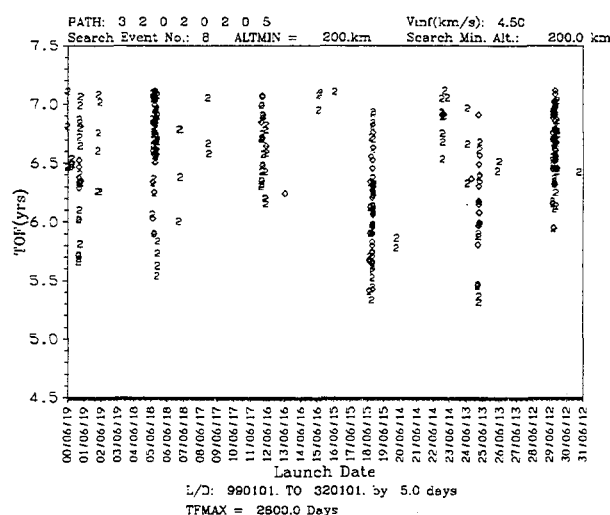


Fig. 2 V^3 trajectories with two V_∞ -leveraging maneuvers (combined $\Delta V \leq 1.25$ km/s).

launch opportunities occur relatively frequently — at least every two to three years, typically. This is readily seen from the launch-date plots produced using STOUR. For example, Fig. 1 shows TOF versus launch-date for low launch energy VEEGAs. Each numeral on the plot represents a trajectory with a certain launch energy, as is explained more fully in Table 1. Such plots serve to identify families of trajectories, and are thus useful for observing trends. Specific trajectories can be chosen from a family by focusing on a smaller date range to make the numerals more discernible if necessary. Another example of a launch-date plot is shown in Fig. 2 for V^3 trajectories with leveraging maneuvers between both Venus pairs. In this case each numeral on the plot represents a certain total deep-space ΔV .

While the classical trajectories are frequently available, non-classical trajectories must also be studied, not only to fill the gaps in the launch-date space, but also to determine any instances where they are superior to the classical options.

Identification of Non-classical Paths

There are several approaches one might take in determining which non-classical paths may be effective. The first approach we employed was to seek variations on the classical paths. One such variation uses a gravity assist at another planet to achieve a V_∞ -leveraging effect. This technique is used, for example, by Sims *et al.*²⁴ Thus, we use such paths as VMV² and VEME where Mars is the leveraging body. Another type of variation on classical paths is the simple addition of another gravity-assist body while outward

Table 1 Legend for launch-date plots

PATH	Planets encountered, including launch and destination bodies, <i>e.g.</i> PATH: 3 2 3 3 5 is a VEEGA from Earth to Jupiter. Maneuvers represented by 0.
Vinf	Launch V_∞ s. Without maneuvers present, the numerals 0, 2, 3, 4, ... on the plot represent the 1 st , 2 nd , 3 rd , 4 th , ... V_∞ s in the list. (0 is used, rather than 1, for better discrimination.) <i>E.g.</i> in Fig. 1 the numeral 3 on the plot denotes a V_∞ of 3.50 km/s. With maneuvers, only one launch V_∞ is shown, as in Fig. 2, where a \diamond represents a ΔV between 0 and 1 km/s, a 2 represents 1 to 2 km/s, <i>etc.</i>
Search Event No.	Event in PATH for which data are plotted. <i>E.g.</i> in Fig. 2, TOF to Jupiter is plotted since encounter with Jupiter is the 8 th event in the PATH.
ALTMIN	Minimum flyby altitude permitted in the STOUR run.
Search Min. Alt.	Trajectories with flyby altitudes below this value are not included in the plot.
L/D	Launch-date range (YYMMDD) used in the STOUR run. <i>E.g.</i> 990101 means 1 Jan. 1999. The launch-date increment is also given, for example “by 5 days.”
TFMAX	Maximum allowable time of flight in the STOUR run.

bound for Jupiter. Examples include VEM and V²E. There is also the obvious insertion of a Mars flyby on a direct Earth-to-Jupiter trajectory. These variations may be used in combination, to yield such paths as VMVE. Another variation is the repetition of a classical type, as in VEVE. A more radical variation is the substitution of Mars for Venus, giving such paths as ME, ME², and M².

The natural concern in devising these paths is the frequency of launch opportunities. STOUR has been our workhorse in addressing this concern; we also discuss some specific cases in a later section. However, it should be noted that intuition regarding the frequency may be misleading — for example, there is no obvious reason why VMV² occurs far less frequently than VEME, yet this is what the STOUR results indicate.

Another approach to pathfinding is to simply list all possible combinations and judiciously rank the list. The restrictions on the paths considered (Venus, Earth, and Mars flybys with a limit of 4 flybys) leaves a complete list of 120 unique paths. Cutting the 120 paths down to a useable number requires intuition and experience. To aid our intuition, we created

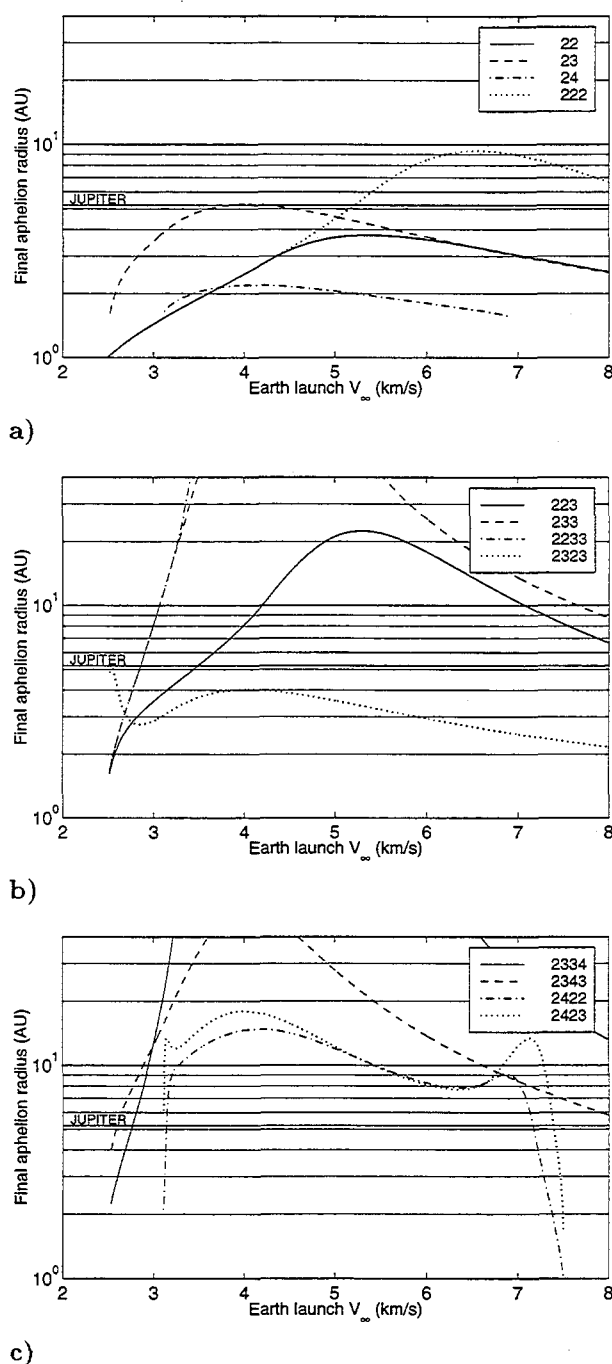


Fig. 3 Gravity Assist Potential plots.

Gravity Assist Potential (GAP) plots for each path. For these plots we assume that the trajectories are ballistic (*i.e.* there are no deep-space maneuvers), the launch from Earth is always tangential, the planetary orbits are circular, and there is no overturning. (The V_∞ vector is turned as much as possible without turning past alignment with the velocity vector of the flyby planet.) For multiple flybys, such as

VM²V, the V_∞ vector is turned in a positive sense at the first Venus (toward alignment with Venus's velocity vector) because the next planet in the path is "outward" (*i.e.* more distant from the Sun). At the second planet, Mars, the V_∞ vector is turned in a negative sense (against alignment with Mars' velocity vector) because the next planet is the same (Mars) and the planet after that (the last Venus) is "inward." In other words, if the next different planet is inward, the V_∞ vector is turned negatively, if it is outward, the V_∞ vector is turned positively. Of course, at the last planet in every path the V_∞ vector is turned in a positive sense to maximize the final aphelion radius. Flyby altitudes as low as 200 km are permitted. The GAP plots associated with some of the paths considered for this paper can be seen in Fig. 3. (For comparison, the minimum V_∞ for a direct launch to Jupiter is 8.79 km/s.) It should be mentioned that when the GAP plots reach their peak aphelion, it is better to use any extra ΔV as a maneuver, rather than for launch V_∞ . We also note that since these GAP plots only apply to ballistic trajectories, they cannot be used to analyze ΔV -EGA trajectories. (A detailed analysis of the ΔV -EGA is provided by Sims²³ and Sims *et al.*²⁴) Another point to make about these plots is that we assume the planets will always be in the right place at the right time (*i.e.* phasing issues are ignored). The GAP plots only indicate feasibility from an energy standpoint.

In Fig. 3, the GAP plots show some interesting characteristics for certain trajectory paths. (The paths in this figure are represented numerically; a VEE is denoted by 233.) The V² path (22 in Fig. 3a) and VM path (24 in Fig. 3a) show that, using these paths alone, it is impossible to get to Jupiter. It is generally true that the V² needs some ΔV to get to Jupiter. In the VM case, STOUR confirms that there are no opportunities with flyby altitudes of 200 km or greater. The VEEGA, well known for its effectiveness, climbs through the Jupiter line before a V_∞ of 3 km/s is reached. A somewhat surprising result is that the V²E reaches Jupiter with a launch V_∞ of 3.5 km/s (Fig. 3b). STOUR confirms that this path in fact exists and that it occurs quite often with launch V_∞ s greater than or equal to 4 km/s. Finally, the V²E² (Fig. 3b) and the VE²M (Fig. 3c) paths show great potential, both reaching Jupiter with a launch V_∞ of less than 3 km/s. As might be expected from the V²E discussion, STOUR shows that the V²E² is an effective trajectory. On the other hand, the VE²M, while exhibiting tremendous potential, does not line up often. When the planets are aligned properly, however, it can be a very efficient trajectory. Further validation of the GAP

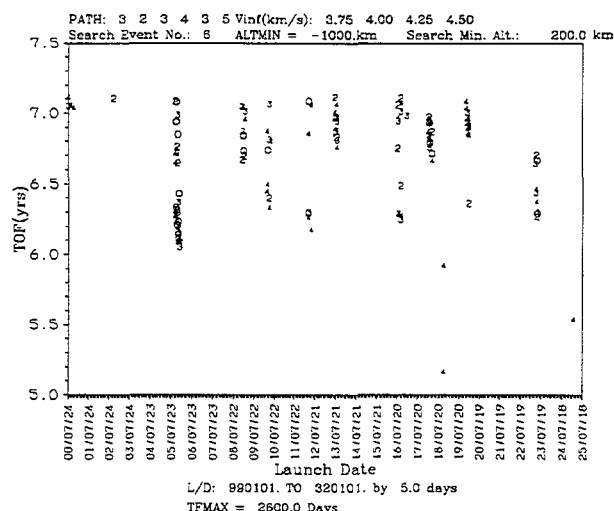


Fig. 4 VEME trajectories.

plots can be seen in Figs. 4 and 5. These figures are STOUR plots of the VEME and VMVE paths. The GAP plots predict that these paths should be able to reach Jupiter with low launch V_{∞} s. The STOUR plots do in fact confirm this. An interesting characteristic of the VMVE plot is the very low TOF case in 2021 (*i.e.* 3.6 yrs). Also notable, is that the path V^2E has a comparable TOF (about 3.7 yrs) in the same year. (VMVE is simply a V^2E that uses Mars as a leveraging body.) The planets align almost perfectly in this year.

Of course, there are some problems with the GAP plots. One drawback is in the assumption to always turn the V_{∞} vector as much as possible without overturning. In a case such as VEVE, the final aphelion radius is greater if, at the first Earth flyby, the V_{∞} vector is turned only enough, or just a little more than enough, to get to the next Venus. The GAP plots indicate that this is a trajectory that cannot reach Jupiter when, in actuality, the STOUR runs show that it is very effective. The GAP plots indicate that some paths do not even exist (see Table 2), because one of the planets in the sequence cannot be reached. However, these paths do in fact exist if we lift our limiting assumptions. Of course, if these simple assumptions prevent a GAP plot from existing, this is a good indication that the particular path is not very useful. As mentioned above, we use the GAP plots to reject some of the 120 possible paths. We eliminate 40 of the paths right away because they have Earth as the first flyby planet. This is just the case of having a ΔV -EGA before one of the other paths. Although the GAP plots give a lot of insight, they tend to be conservative in that they eliminate only 41 trajectory paths in addition to the 40 mentioned above. Table 3 gives a list of the 39 paths that

Table 2 Paths that have no GAP plot

MV	MVV	MVE	MVM	MMV
MVVV	MVVE	MVVM	MVEV	MVEE
MVEM	MVMV	MVME	MVMM	MEMV
MMVV	MMVE	MMVM	MMMV	

Table 3 Paths reaching Jupiter, based on GAP analysis

M	VE	ME	MM	VVV
VVE	VEE	VEM	MEE	MEM
MME	MMM	VVVV	VVVE	VVVM
VVEE	VVEM	VVMV	VVME	VVMM
VEVE	VEEE	VEEM	VEMV	VEME
VEMM	VMVV	VMVE	VMEE	MEVV
MEVE	MEEE	MEEM	MEME	MEMM
MMEE	MMEM	MMME	MMMM	

reach Jupiter with a launch V_{∞} less than 8 km/s.

Investigation of a Selected Set of Paths

Due to the long computation time that would be needed to run all of the 120 flyby combinations in STOUR, we limited our search to a "selected set" of paths, which are listed in Table 6. This selected set comprises all of the classical paths, and most of the non-classical paths which appeared to be reasonable candidates. These candidates are identified using the two approaches discussed in the previous section, in conjunction with engineering intuition regarding time of flight and orbit geometry. For example, the GAP plots indicate that M^2 , V^3 , and VE^2 all reach Jupiter; thus, adding an extra encounter of the last flyby body would probably have little effect on the launch energy, while making the time of flight prohibitively long. Thus there is no need to study M^3 , V^4 , and VE^3 . Other paths, such as M^2E , are unattractive because the double Mars encounter, when best used, raises perihelion above Earth's orbit. This eliminates all paths starting with M^2E . Some paths, such as VEVE, are included since they seem to be viable variations of classical types, in spite of their poor performance under the assumptions of the GAP analysis. Also, one 5-flyby path, VMVMV, is considered due to its dramatic potential for two leveraging-effect gravity assists. Finally it should be noted that Table 6 does not contain all reasonable non-classical types, for example, V^3E , V^3M , and MEM are missing. These and other paths were rejected because they were deemed less likely to produce many viable results with acceptable TOFs, and because of the time-intensive searches

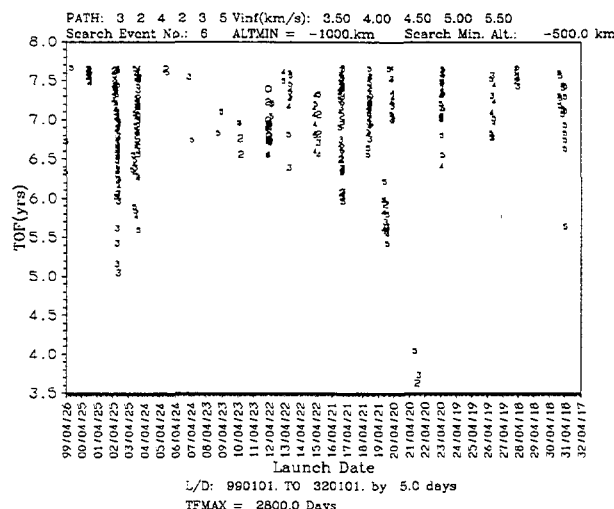


Fig. 5 VMVE trajectories.

involved. For the same reason, an assessment of leveraging with STOUR was made only for the V^2 , V^3 , VEEGA and ΔV -EGA trajectories of Table 6.

The paths in the selected set were first examined over the whole launch period (1 January 1999 to 31 December 2031) using STOUR. To present this enormous amount of data, we divide the paths into two groups, depending on whether Earth is used as a flyby body. (In missions utilizing radioisotope power sources, we can reduce the risk of Earth impact by not using Earth as a gravity-assist body.) For each group we list up to three of the most attractive trajectories in each calendar year (see Tables 4 and 5). In making our selections for each year, we sought low TOF with 1) low deep-space ΔV (or above-surface flybys), 2) low launch V_∞ , and 3) low arrival V_∞ . Of course, some sort of trade was typically involved between these quantities. As a rough rule of thumb, these quantities are listed in decreasing priority. Approximately speaking, an extra 0.5 to 1 km/s in launch V_∞ , or up to 0.5 km/s in deep-space ΔV , would only be accepted if it reduced TOF by at least a year. At the other end of the spectrum, increases of 0.5 to 2 km/s in arrival V_∞ would be accepted even if TOF was decreased by only 0.5 to 1 years. Sometimes, especially when these quantities changed simultaneously, rather than choosing between several good candidates, up to three were listed, as for the year 1999 in Table 4, or 2031 in Table 5. A similar selection approach was taken in evaluating the best that each path had to offer over the whole launch period. These unoptimized trajectories are shown in Table 6. We note that each trajectory listed in the tables is typically a member of a trajectory family that can show significant variation in the key quantities near the same launch date. Thus, for example, mission designers wanting to use Jupiter as a gravity-

assist body for exploration of the outer solar system should usually be able to find similar trajectories to those listed, but with higher arrival V_∞ s.

Optimized versions of the Table 4 and Table 5 trajectories up to 2010 are shown in Table 7, along with several noteworthy trajectories after 2010. The optimization, performed using MIDAS,²¹ was of launch ΔV plus deep-space ΔV . (Flyby times and other data are listed in these tables to facilitate recreation of the trajectories.) A comparison of the optimized with the unoptimized trajectories demonstrates the relatively close correspondence between the two. One factor which affects this correspondence is the granularity of the search in STOUR — the size of the increments in launch V_∞ and launch date. The latter was always taken as 5 days, while the former was typically 0.25 km/s (*e.g.* for the VEEGAs) or 0.5 km/s (*e.g.* for the V^3 s), although 1 km/s was used for some of the less interesting paths, such as V^2M . In some cases, particularly those involving leveraging, the optimized solution was considerably better than the unoptimized, due to the fact that STOUR does not try to optimize the leveraging maneuver for each specific trajectory; it merely shows that a feasible leveraging family exists at a particular time.

It is immediately obvious that the classical VEEGAs, VEGAs, and V^3 s dominate the trajectory tables. This indicates that the attention given to these trajectories by other researchers, such as Diehl and Myers,¹⁵ was well placed. A somewhat surprising result is that the well-known ΔV -EGA does not perform well enough to appear in Table 4. Another general observation is that the best trajectories involving Earth flybys are significantly better than the best of the no-Earth-flyby trajectories, by almost any performance measure. This again corresponds well with the choice by Diehl and Myers to examine only VEGAs and VEEGAs.

The classical trajectories exhibit some unexpected resonance characteristics. While most of the VEEGAs have around two years between Earth flybys as expected, the 99-06-25 and 14-11-23 cases of Table 4 exhibit a three year resonance. Roughly half of the V^3 s in Table 5, resonant and non-resonant, have about 2 Venus years between the first two Venus flybys, and about 4 between the last two, which we denote by $[\sim 2; \sim 4]$. Roughly half are $[\sim 2; \sim 3]$. Two trajectories, in 2004 and 2023, manage to achieve a 5 Venus-year resonance. Surprisingly, there are two instances of a $[\sim 3; \sim 3]$, where the “=” denotes an exact resonance, in 2006 and 2019; these are among the worst of the listed V^3 s. In contrast, the V^3 s listed in Table 6 are both $[\sim 2; \sim 3]$, due to their slightly shorter flight times.

Table 4 Promising trajectories including Earth flybys (unoptimized)

Path	Launch Date	Launch V_{∞} , km/s	Flyby Alt., ^a km or ΔV , ^a km/s	Arrival V_{∞} , km/s	TOF, yrs	Flyby Times, ^b days after launch
VE	99-03-27	4.50	.314(2)	5.79	5.1	339,947
VEE	99-05-21	3.00	.395(2)	5.90	5.8	155,438,1259
VEE	99-06-25	3.75		5.77	7.0	178,492,r,1588
VEE	00-08-23	3.50	.070(2)	6.53	6.6	374,754,1590
VEE	01-02-24	3.75		5.82	6.6	173,693,r,1424
VEE	02-07-15	3.50		6.07	5.9	145,633,1256
VEE	03-11-07	4.00		6.62	6.5	383,776,1623
VE	04-05-04	4.50	.794(2)	5.97	4.4	140,652
VEE	04-06-17	5.00		6.55	6.0	155,680,r,1410
VEE	05-10-12	3.50		6.65	5.6	162,476,1300
VE	06-12-10	4.50	.868(2)	6.32	5.1	433,835
VEE	07-02-24	4.00		6.56	6.5	359,772,1631
VEE	08-12-09	4.00		6.71	5.7	152,634,r,1365
VEE	09-01-24	3.75		5.60	6.1	167,484,1315
VEME	10-04-18	4.00		8.27	6.4	365,936,1512,1680
VEE	10-07-17	3.00	.431(2)	6.21	6.6	133,753,1568
VEE	11-09-20	4.25		5.99	7.6	416,777,r,1508
VEE	12-04-13	3.50		5.88	6.1	181,498,1329
VEE	13-10-29	4.00		5.68	6.0	91,401,r,1131
VEE	14-11-23	4.00		7.16	7.3	442,825,r,1921
VEVE	14-11-28	4.50		8.49	7.0	439,999,1289,1880
VEE	15-05-27	3.75		6.74	5.9	148,655,r,1386
VE	16-09-18	4.50	.255(2)	6.20	5.1	349,924
VEE	17-01-06	3.75		6.64	6.5	134,448,r,1179
VE	18-07-25	4.50	-377,-40(1,2)	8.58	4.5	421,1051
VEE	18-09-08	3.50		6.03	6.6	160,679,r,1410
VMVE	19-10-23	4.00	-172(4)	7.43	5.6	433,1024,1350,1400
VEE	20-03-26	3.00		6.75	6.4	171,506,r,1601
VEE	20-04-05	3.50		6.22	5.4	156,455,r,1186
VMVE	21-10-27	4.00	-346(4)	7.32	3.6	148,275,608,663
VVEE	21-11-13	3.50		6.86	7.1	173,616,1087,r,1818
VVE	22-01-20	5.00		6.68	5.9	171,563,1390
VEME	23-05-30	3.25		5.58	6.4	146,461,623,1276
VEE	24-08-28	3.50		6.08	6.8	371,942,1538
VEE	25-02-23	4.00		6.60	6.1	177,699,r,1429
VEM	26-06-13	4.25	+183(3)	5.75	5.2	431,871,1007
VEEM	26-08-09	3.00		7.34	6.5	105,577,r,1672,1748
VE	27-10-16	5.00	-124(2)	6.09	4.8	390,792
VEE	28-03-09	3.50	.697(2)	6.09	6.6	121,746,1460
VE	28-03-19	4.50	.699(2)	6.05	4.6	201,712
VEE	29-11-05	3.25		6.40	5.6	146,464,1291
VEVE	30-12-24	4.50		7.63	6.3	422,824,913,1607
VEE	31-04-23	3.25	.674(2)	6.81	6.2	170,817,1529
VE	31-07-17	4.50	.690(2)	6.39	4.1	180,701

^aOnly flyby altitudes below 200 km are listed; they are prefixed with a + or - sign. The parenthetical numbers indicate the associated flyby number. Deep-space ΔV s, if present, are listed without a prefixed sign; the parenthetical numbers indicate the flyby number preceding the maneuver.

^bAn "r" between the flyby times indicates that resonance occurs on that leg.

In spite of the success of the classical paths, the non-classical paths play three roles: They occasionally provide advantages even over the best classical trajectory; they sometimes improve on a classical tra-

jectory in the same year; and lastly, they may provide trajectories in years where no viable classical trajectories exist. The first role is exemplified by the 2021 VMVE trajectory shown in Tables 4 and 7. Its flight

Table 5 Promising trajectories without Earth flybys (unoptimized)

Path	Launch Date	Launch V_{∞} , km/s	Flyby Alt., ^a km or ΔV , ^a km/s	Arrival V_{∞} , km/s	TOF, yrs	Flyby Times, ^b days after launch
VMVV	99-04-26	5.50		6.49	6.7	322,616,850,r,1524
VVV	00-08-23	4.50	1.17(1)	6.99	6.3	365,860,1478
VVV	01-02-24	4.50	.145,.230(1,2)	7.33	6.4	187,638,1548
VVV	01-04-22	6.00		7.21	6.3	397,772,1497
VVV	02-08-23	6.00	+177,+17(1,3)	7.60	5.5	70,r,519,1246
VMVV	03-11-26	4.00		8.15	7.2	370,715,1243,1974
VVV	04-07-15	6.00		7.18	6.9	168,r,617,r,1741
VVV	05-10-31	4.50	.519,.039(2,3)	7.16	5.6	85,580,1270
VVV	06-01-29	7.00	-280(3)	6.82	6.9	382,963,r,1637
VVMV	07-04-14	5.00		7.07	6.9	324,r,774,895,1433
VVV	07-10-27	6.50		7.52	6.0	142,r,592,r,1491
VVV	08-12-04	4.50	.338,.683(1,2)	7.11	7.1	435,893,1812
VVV	09-02-12	4.50	1.004,.554(2,3)	7.38	7.0	189,595,1246
VVV	10-05-18	4.50	.791,.278,.452(1,2,3)	7.15	6.2	347,786,1510
VVV	11-01-15	6.50	-551(1)	7.28	6.2	154,r,603,r,1502
VMVV	12-04-27	4.00		7.12	7.0	181,799,1101,1708
VVV	13-09-04	6.50		7.37	6.8	327,r,776,1718
VVV	14-04-09	7.00	-394,-366(1,3)	8.98	5.2	143,r,593,r,1267
VVV	15-07-29	6.50		8.94	6.4	418,792,1733
VVV	15-08-10	4.50	.617(2)	7.27	6.7	172,567,1502
VVV	16-12-27	6.00	+177(3)	8.18	6.4	304,r,753,1689
VVMV	17-01-06	4.50	+160(1)	7.02	7.0	136,800,994,1558,1665
VVV	18-10-03	4.50	.403(2)	7.01	5.7	179,581,1289
VVMV	18-10-24	5.00		6.98	5.9	175,570,667,1278
VVV	19-01-11	6.50		6.86	6.1	155,728,r,1402
VVV	20-03-16	6.00	+39(1)	8.46	5.8	79,r,529,1470
VVV	21-11-26	4.50	.338,.522,.649(1,2,3)	7.16	5.7	184,643,1331
VVV	22-03-14	6.50	+33(1)	7.06	6.8	376,748,1692
VVV	22-12-26	4.50	.292,.491,.304(1,2,3)	6.53	6.9	478,945,1641
VVV	23-05-25	5.50		6.97	6.9	83,596,r,1720
VVV	24-08-17	4.50	.857,.390,.043(1,2,3)	7.46	6.2	365,797,1511
VVV	25-03-20	4.50	.138,.244(1,2)	7.14	6.4	173,624,1531
VVV	25-05-12	6.00		10.50	5.6	160,535,1476
VMVV	26-08-07	4.50		7.11	7.2	419,515,795,1748
VMVV	26-08-07	4.50	-34(4)	7.45	6.2	419,515,795,r,1469
M	27-02-08	8.00		5.87	6.5	1563
VVV	27-11-30	4.50	.230,1.097,.176(1,2,3)	7.27	6.7	353,833,1473
VVV	28-07-15	6.00		7.32	6.9	165,r,614,r,1513
VVV	29-10-15	4.50	.396(2)	7.12	6.2	414,815,1524
VVV	30-12-19	4.50	.453,.893(1,2)	8.64	6.0	399,884,1579
M	31-02-12	8.00		6.20	2.3	96
VMVV	31-04-23	5.50	+142(4)	7.33	7.2	317,528,755,r,1429

^aOnly flyby altitudes below 200 km are listed; they are prefixed with a + or - sign. The parenthetical numbers indicate the associated flyby number. Deep-space ΔV s, if present, are listed without a prefixed sign; the parenthetical numbers indicate the flyby number preceding the maneuver.

^bAn "r" between the flyby times indicates that resonance occurs on that leg.

time is not even 1 year greater than that of a classical Hohmann transfer, while the launch V_{∞} is less than half that of the Hohmann, and only minimal deep-space ΔV is needed. An instance of the second role is the 2023 VEME (Tables 4, 6 and 7), whose launch V_{∞} is 0.5 km/s less than the nearest VEEGA

competitor, and whose TOF is also somewhat less. Similarly, the VMV² in 2012 (Tables 5 and 6) is significantly better than any 2012 V³. An example of the third role is the V²E in 2022 (Table 4), a year where there are no VEGAs or VEEGAs of the typical sort. (The only comparable VEEGA in 2022 has sim-

Table 6 The best candidate(s) for each path (unoptimized)

Path	Launch Date	Launch V_{∞} , km/s	Flyby Alt., ^a km or ΔV , ^a km/s	Arrival V_{∞} , km/s	TOF, yrs	Flyby Times, ^b days after launch
E	04-02-24	5.21	.875(0)	6.54	4.1	678
E	14-03-03	5.22	.585(0)	5.81	6.7	1411
M	31-02-12	8.00		6.20	2.3	96
VV	31-08-06	5.00	.376,1.160(1,2)	7.04	4.2	178,633
VV	31-08-14	5.00	1.493(2)	7.24	4.5	174,r,624
VE	05-10-01	4.50	.179(2)	6.38	5.1	416,859
VE	15-07-06	4.00		7.62	6.2	177,891
VM	<i>No feasible trajectories</i>					
MV	<i>No feasible trajectories</i>					
ME	12-08-05	5.50		5.60	5.0	640,837
ME	26-11-15	6.00		8.94	3.9	145,777
MM	18-05-19	7.00		5.42	6.3	78,r,1452
VVV	01-04-22	6.00		7.21	6.3	397,772,1497
VVV	18-10-03	4.50	.403(2)	7.01	5.7	179,581,1289
VVE	20-03-08	4.00		6.03	5.9	103,592,1175
VVM	03-09-07	7.75	-964(1)	6.60	5.5	408,r,1082,1180
VEV	<i>No feasible trajectories</i>					
VEE	29-11-05	3.25		6.40	5.6	146,464,1291
VEM	26-06-13	4.25	+183(3)	5.75	5.2	431,871,1007
VMV	05-10-31	5.50	-266,-604(1,3)	7.13	6.6	404,834,1479
MVM	<i>No feasible trajectories</i>					
MEE	00-12-21	5.00		8.06	7.0	746,1127,r,1858
VVEE	18-09-17	3.50		7.09	6.8	159,r,609,1041,r,1772
VVMV	18-10-24	5.00		6.98	5.9	175,570,667,1278
VEVE	26-08-27	3.50		8.27	6.3	176,695,1043,1590
VEEM	26-08-09	3.00		7.34	6.5	105,577,r,1672,1748
VEME	23-05-30	3.25		5.58	6.4	146,461,623,1276
VMVV	12-04-27	4.00		7.12	7.0	181,799,1101,1708
VMVE	21-10-27	4.00	-346(4)	7.32	3.6	148,275,608,663
VMVMV	17-01-06	4.50	+160(1)	7.02	7.0	136,800,994,1558,1665

^aOnly flyby altitudes below 200 km are listed; they are prefixed with a + or - sign. The parenthetical numbers indicate the associated flyby number. Deep-space ΔV s, if present, are listed without a prefixed sign; the parenthetical numbers indicate the flyby number preceding the maneuver, with 0 signifying Earth launch.

^bAn "r" between the flyby times indicates that resonance occurs on that leg.

ilar launch energy — uncharacteristically high for a VEEGA — but slightly worse arrival V_{∞} and TOF.)

It is interesting to note that while Mars can be frequently used as a leveraging body for the VEEGAs (see Fig. 4), it seldom improves performance, as witnessed by the dearth of VEME trajectories in Table 4. On the other hand, Mars is much less often available as a leveraging body with the V^3 s, but when it is available, it is very efficacious (see Table 5). Also, it is seen that VMV^2 trajectories are more effective than V^2MV . One reason for this is that with the VMV^2 there are two Venus flybys available to turn the increased V_{∞} , rather than just one. Mars need not always be used as a leveraging body. For example, it can be used in 2031 to improve on the classical Hohmann transfer, in terms of both TOF and launch energy.

For many of the non-classical paths, the optimal relative alignment of the planets does not recur often. The Mars gravity assist recurs every 47 to 49 years. The remarkable 2021 VMVE repeats in similar form about every 45 years, although a slight shift occurs after the beginning of the 22nd century. For this path, the relative orientations of 2021 are sometimes not repeated as precisely as those of the 2031 Mars gravity assist. This might be expected, because it involves the realignment of four planets, not just three, whose periods are not in simple ratios to each other.

Conclusions

We have taken a systematic approach to the identification of low-energy, gravity-assist trajectories to Jupiter with launch opportunities in the next three

Table 7 Optimized trajectories

Path	Launch Date	Launch V_{∞} , km/s	Deep-space ΔV , km/s	Arrival V_{∞} , km/s	TOF, yrs	Flyby Times, ^a days after launch
VE	99-03-27	4.50	.298	5.80	5.1	339,947
VEE	99-05-16	3.03	.276	6.10	5.8	157,438,1257
VEE	99-06-09	3.37	0	5.55	7.3	175,513,r,1608
VEE	00-08-11	3.07	0	6.55	6.6	387,766,1604
VEE	01-02-24	3.75	0	5.82	6.6	173,693,r,1423
VEE	02-07-23	3.40	0	6.56	5.7	140,624,1247
VEE	03-11-19	3.80	0	6.62	6.5	373,764,1610
VEE	04-03-12	3.56	.471	6.36	6.3	122,740,r,1470
VE	04-04-23	4.14	.719	6.03	4.3	145,663
VEE	05-10-28	3.14	0	6.65	5.6	153,458,1282
VE	06-12-16	4.05	.813	6.20	4.9	429,822
VEE	07-02-28	3.93	0	6.56	6.5	355,768,1626
VEE	08-12-09	4.02	0	6.70	5.7	152,634,r,1364
VEE	09-01-21	3.68	0	5.50	6.3	172,488,1320
VEE	10-04-06	3.69	0	8.27	6.4	377,947,1523,1692
VEE	10-07-21	2.94	.360	6.21	6.6	129,747,1560
VMVV	99-04-27	5.46	0	6.49	6.7	320,615,848,r,1522
VVV	00-08-04	2.97	.734	6.62	6.6	393,825,1523
VVV	01-03-04	3.89	.360	7.33	6.4	173,r,628,r,1539
VVV	01-04-24	5.93	0	7.24	6.3	394,770,1494
VVV	02-08-25	4.54	.438	7.92	5.4	77,527,1244
VMVV	03-12-01	3.94	0	8.05	7.2	365,710,1237,1968
VVV	04-07-09	5.34	.037	8.60	6.5	162,r,611,r,1737
VVV	05-10-30	4.20	.508	7.45	6.3	89,576,1278
VVV	06-01-04	5.34	.171	6.83	7.0	403,991,r,1660
VVMV	07-04-09	4.87	0	7.06	6.9	329,r,779,900,1438
VVV	07-10-10	5.78	.011	8.36	5.9	155,r,605,r,1503
VVV	08-12-01	4.26	.608	7.56	6.9	430,r,888,r,1805
VVV	09-02-21	3.77	1.044	7.36	7.0	173,565,r,1240
VVV	10-05-19	4.28	1.098	6.42	7.0	349,837,1483
VVMV	18-11-02	4.67	0	7.05	6.1	164,563,660,1267
VMVE	21-10-27	3.99	.425	6.90	3.7	148,275,607
VEE	23-05-28	3.25	0	5.58	6.4	147,463,624,1278
VEEM	26-08-03	2.93	0	7.34	6.6	110,582,r,1678,1753
M	31-02-15	7.84	0	5.83	2.5	95

^aAn "r" between the flyby times indicates that resonance occurs on that leg.

decades. Starting from a list of all possible combinations of up to four flybys with Venus, Earth, and Mars, we used energy considerations, estimates of time of flight, and engineering judgement to reduce the number of paths to a selected set of 25 cases. We then employed an automated design program to calculate all occurrences of each path for the 33-year launch period. We also identified the ΔV -optimal paths for the first decade.

While we make no claim that these are global optimal solutions, we believe that our results are broadly representative of the effectiveness of both classical and non-classical trajectory paths. The methods we have presented should be applicable in the search for gravity-assist trajectories to other solar system bod-

ies; we hope our trajectories to Jupiter will provide designers with useful benchmarks for future missions to our largest planet.

Acknowledgments

This research has been supported in part by the Jet Propulsion Laboratory, California Institute of Technology under Contract Number 961211. We are grateful to Dennis V. Byrnes (Technical Manager), Jan M. Ludwinski, and Robert W. Maddock for providing useful information, guidance and helpful suggestions. We also thank Nathan J. Strange, a graduate student in the School of Aeronautics and Astronautics at Purdue University, for his assistance.

References

- ¹Broucke, R. A., "The Celestial Mechanics of Gravity Assist," AIAA Paper 88-4220, Aug. 1988.
- ²Battin, R. H., *An Introduction to the Mathematics and Methods of Astrodynamics*, AIAA Education Series, AIAA, New York, 1987, pp. 423-424.
- ³Battin, R. H., "The Determination of Round-trip Planetary Reconnaissance Trajectories," *Journal of the Aero/Space Sciences*, Vol. 26, No. 9, Sept. 1959, pp. 545-567.
- ⁴Sedov, L. I., "Orbits of Cosmic Rockets Toward the Moon," *ARS Journal*, Vol. 30, No. 1, Jan. 1960, pp. 14-21.
- ⁵Deerwester, J. M., "Jupiter Swingby Missions to the Outer Planets," *Journal of Spacecraft and Rockets*, Vol. 3, No. 10, Oct. 1966, pp. 1564-1567.
- ⁶Flandro, G. A., "Fast Reconnaissance Missions to the Outer Solar System Utilizing Energy Derived from the Gravitational Field of Jupiter," *Astronautica Acta*, Vol. 12, No. 4, 1966, pp. 329-337.
- ⁷Gillespie, R. W., Ragsac, R. V., and Ross, S. E., "Prospects for Early Manned Interplanetary Flights," *Astronautics and Aerospace Engineering*, Vol. 1, No. 7, Aug. 1963, pp. 16-21.
- ⁸Hollister, W. M., "Mars Transfer via Venus," AIAA/ION Astrodynamics Guidance and Control Conference, AIAA Paper 64-647, Los Angeles, CA, Aug. 1964.
- ⁹Minovitch, M. A., "The Determination and Characteristics of Ballistic Interplanetary Trajectories Under the Influence of Multiple Planetary Attractions," Jet Propulsion Laboratory, Technical Report No. 32-464, Pasadena, CA, Oct. 1963.
- ¹⁰Niehoff, J. C., "Gravity-Assisted Trajectories to Solar System Targets," *Journal of Spacecraft and Rockets*, Vol. 3, No. 9, Sept. 1966, pp. 1351-1356.
- ¹¹Ross, S., "Trajectory Design for Planetary Mission Analysis," *Recent Developments in Space Flight Mechanics*, edited by P. B. Richards, Vol. 9, Science and Technology Series, AAS, Washington, D.C., 1966.
- ¹²Sohn, R. L., "Venus Swingby Mode for Manned Mars Missions," *Journal of Spacecraft and Rockets*, Vol. 1, No. 5, Sept.-Oct., 1964, pp. 565-567.
- ¹³Sturms, F. M. and Cutting, E., "Trajectory Analysis of a 1970 Mission to Mercury via a Close Encounter with Venus," AIAA Second Aerospace Sciences Meeting, AIAA Paper 65-90, New York, NY, Jan. 1965.
- ¹⁴Stancati, M. L., Friedlander, A. L., and Bender, D. B., "Launch Opportunity Classification of VEGA and ΔV -EGA Trajectories to the Outer Planets," AIAA Paper 76-797, Aug. 1976.
- ¹⁵Diehl, R. E. and Myers, M. R., "Gravity-Assist Trajectories to the Outer Solar System," Jet Propulsion Laboratory, JPL Publication D-4677, Pasadena, CA, Sept. 1987.
- ¹⁶Williams, S. N., "Automated Design of Multiple Encounter Gravity-Assist Trajectories," M.S. Thesis, School of Aeronautics and Astronautics, Purdue University, West Lafayette, IN, Aug. 1990.
- ¹⁷Rinderle, E. A., "Galileo User's Guide, Mission Design System, Satellite Tour Analysis and Design Subsystem," Jet Propulsion Laboratory, JPL Publication D-263, Pasadena, CA, July 1986.
- ¹⁸Patel, M. R., "Automated Design of Delta-V Gravity-Assist Trajectories for Solar System Exploration," M.S. Thesis, School of Aeronautics and Astronautics, Purdue University, West Lafayette, IN, Aug. 1993.
- ¹⁹Patel, M. R. and Longuski, J. M., "Automated Design of Delta-V Gravity-Assist Trajectories for Solar System Exploration," AAS/AIAA Astrodynamics Specialist Conference, AAS Paper 93-682, Victoria, British Columbia, Aug. 1993.
- ²⁰Staugler, A. J., "STOUR (Satellite Tour Design Program) User's Guide for the ΔV -EGA and V_{∞} -Leveraging Routines," Technical Report, School of Aeronautics and Astronautics, Purdue University, West Lafayette, IN, June 1996.
- ²¹Sauer, C. G., "MIDAS: Mission Design and Analysis Software for the Optimization of Ballistic Interplanetary Trajectories," *Journal of the Astronautical Sciences*, Vol. 37, No. 3, July-Sept., 1989, pp. 251-259.
- ²²Hollenbeck, G. R., "New Flight Techniques for Outer Planet Missions," American Astronautical Society, AAS Paper 75-087, July 1975.
- ²³Sims, J. A., "Delta-V Gravity-Assist Trajectory Design: Theory and Practice," Ph.D. Thesis, School of Aeronautics and Astronautics, Purdue University, West Lafayette, IN, Dec. 1996.
- ²⁴Sims, J. A., Longuski, J. M., and Staugler, A. J., " V_{∞} Leveraging for Interplanetary Missions: Multiple-Revolution Orbit Techniques," *Journal of Guidance, Control, and Dynamics*, Vol. 20, No. 3, May-June, 1997, pp. 409-415.